Supporting Information for

Nanoscale carrier multiplication mapping in a Si diode

Corentin Durand, Pierre Capiod, Maxime Berthe, Jean-Philippe Nys, Christophe Krzeminski, Didier Stiévenard, Christophe Delerue, Bruno Grandidier*

Institut d'Electronique, de Microélectronique et de Nanotechnologies (IEMN), CNRS, UMR 8520 Département ISEN, 41 bd Vauban, 59046 Lille Cedex, France

* B. Grandidier. E-mail: bruno.grandidier@isen.iemn.univ-lille1.fr

1) Materials and methods

The Si diodes were built in a *n*-type (100) silicon wafer (arsenic doped 4.5 x 10^{16} atoms.cm^{-3}). p^{++} regions, with a width of 1.0 µm and lengths varying between 0.2 and 1.0 µm, were first patterned (see Figure S1) and boron impurities were implanted with a dose of 5.0 x 10^{15} atoms.cm^{-2} at an energy of 30 keV. The PMMA resist was removed by immersing the sample in a SVC-14 bath that was followed by an oxygen plasma treatment. The n^{++} regions, with similar sizes, were subsequently patterned at a distance of 1 µm from the p^{++} regions and arsenic impurities were implanted with a dose of 5.0 x 10^{15} atoms.cm^{-2} at an energy of 140 keV. The PMMA resist was again removed with the same procedure. Finally, the sample was dipped in a Piranha solution (1/2 mixture of H_2SO_4/H_2O_2) and the native oxide was etched with an aqueous ammonium fluoride solution degassed under nitrogen flow.[1] Based on the SEM observations of the diodes as the ones shown in Figures 1b, 3a and S1, we generally found a corolla around the n^{++} region, that is attributed to surface contamination by the resist that was irradiated with highly energetic ions. In order to prepare a surface compatible with scanning tunneling microscopy, the sample was further annealed by Joule heating at a temperature of 850°C for 30 minutes in ultra high vacuum (UHV), what simultaneously allows for dopant activation and removal of the surface oxyde layer.

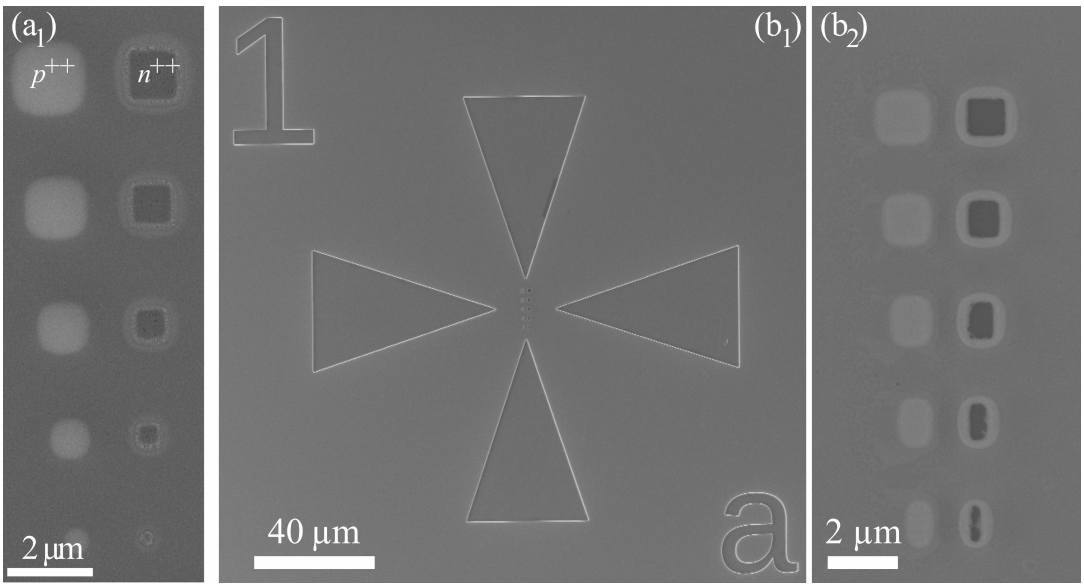

Figure S1: SEM images of two sets of Si diodes that were characterized in this work. The diodes shown in these images have either a square (a) or (b) rectangular geometry. Figure (b1) shows the microscopic marks that are used to easily locate the diodes.

In order to estimate the doping level resulting from the implantation activation and diffusion steps in each region, process simulations based on 2D numerical finite elements methods have been achieved with the Taurus Process software.[2] They are classically based on a statistical method which estimates the penetration of the implanted ions into the implanted layer and the related damage.[3] A large number of particules events (200 000) have been assumed to reach a generated realistic profile. In order to take into account the influence of the annealing step performed in UHV on the dopant junction profile, classical diffusion models for the boron and arsenic impurity diffusion have been considered. The resulting doping profile is shown in Figure 1c. The p^{++} and n^{++}-type regions are degenerated, allowing the formation of ohmic contact with tips 1 and 2 and the formation of an abrupt p^{++}-n junction. The abruptness of the junction is confirmed by measuring current versus voltage characteristics, that exhibits a good rectifying behaviour (Figure 1d).

The experiments were performed with a four-probe scanning tunneling microscope combined with a scanning electron microscope in UHV at a pressure lower than $2x10^{-10}$ Torr (Nanoprobe system, Omicron Nanotechnology). All four STM tips are simultaneously and independently operated with a dedicated control system (Nanonis SPECS). Prior to their use in the analysis chamber, the W tips were thoroughly cleaned by direct resistive heating and their radius was controlled in field emission in the preparation chamber. The procedure to bring tips 1 and 2 in contact with the sample consists, first, in performing STM images of the p^{++} and n^{++} regions with tip 1 or tip 2, then, in immobilizing the tips on clean areas, third, in opening the feedback loop and derivating the current to another amplifier with a lower gain and, finally, in approaching the tips. The current characteristics at constant voltage shows an exponential increase with decreasing tip-sample distance until a saturation is reached, indicating the establishment of the electrical contact.[4]

2) Comparison between BEEM and multiple probe STM in the determination of the quantum yield.

As stated in the introduction of the paper, an accurate measurement of the quantum yield for impact ionization is not straightforward and might be fraught with incertainty. Indeed, the BEEM technique is based on a three-terminal configuration: a tip, a thin metal electrode at the top of a semiconductor surface and the semiconductor material. Two currents are measured: the tunneling current from the tip to the metal base electrode, that leads to the injection of ballistic electrons into the base electrode, and the collector current that flows between the metal base electrode and the semiconductor collector. Likewise the multiple probe STM technique, the feedback loop is active during the spectroscopic measurement. When the bias applied between the tip and the metal base electrode is high enough, impact ionization occurs in the semiconductor.[5] The generated charge carriers are separated by the electrical field of the Schottky barrier at the interface between the metal and the semiconductor. The generated electrons and the ballistic electrons are collected by the semiconductor collector, whereas the holes drift to the metal base where they recombine with the tunneling electrons. Therefore, the BEEM technique can only collect one type of free charge carriers generated by the ballistic electrons. Then, in the BEEM technique, part of the tunneling electrons scatters in the metal base electrode and does not reach the collector. As a result, the number of incident electrons transferred into the collector is always smaller than the total number of tunneling electrons. In Ref 5, the ratio between the incident electrons reaching the semiconductor and the total number of tunneling electrons was ~0.75 at a voltage of 2V. This ratio should increase at higher bias due to finite width of the energy distribution of the injected electrons, but should always be smaller than one. Therefore, the BEEM technique overestimates the quantum yield.

3) Discussion about the tunneling tip influence on the experiments

The proximity of the tip and its electronic property causes the following effects:

- There is some uncertainty in the quantification of the incident tunneling electrons. Indeed, the energy distribution of the incident electrons has a finite width. As a result, in the vicinity of the threshold voltage, not all the incident electrons have enough energy to give rise to impact ionization. Because the energy distribution width is less than 0.2 eV at room temperature,[6] this effect can be neglected in the determination of the quantum yield.

- At a tip voltage high enough, when the tip Fermi level reaches the vacuum level of the semiconductor, field emission resonances occur. They affect the transmission probability through the tunneling barrier, but not the generation of electron-hole pairs. This effect is seen in Figure S2b: a stronger increase of tip-sample separation takes place at a voltage of 6.5 V. However, in this voltage range, there is no significant variation of the electron and hole currents as shown by the position of the vertical dashed line. The threshold for CM occurs at lower voltages.

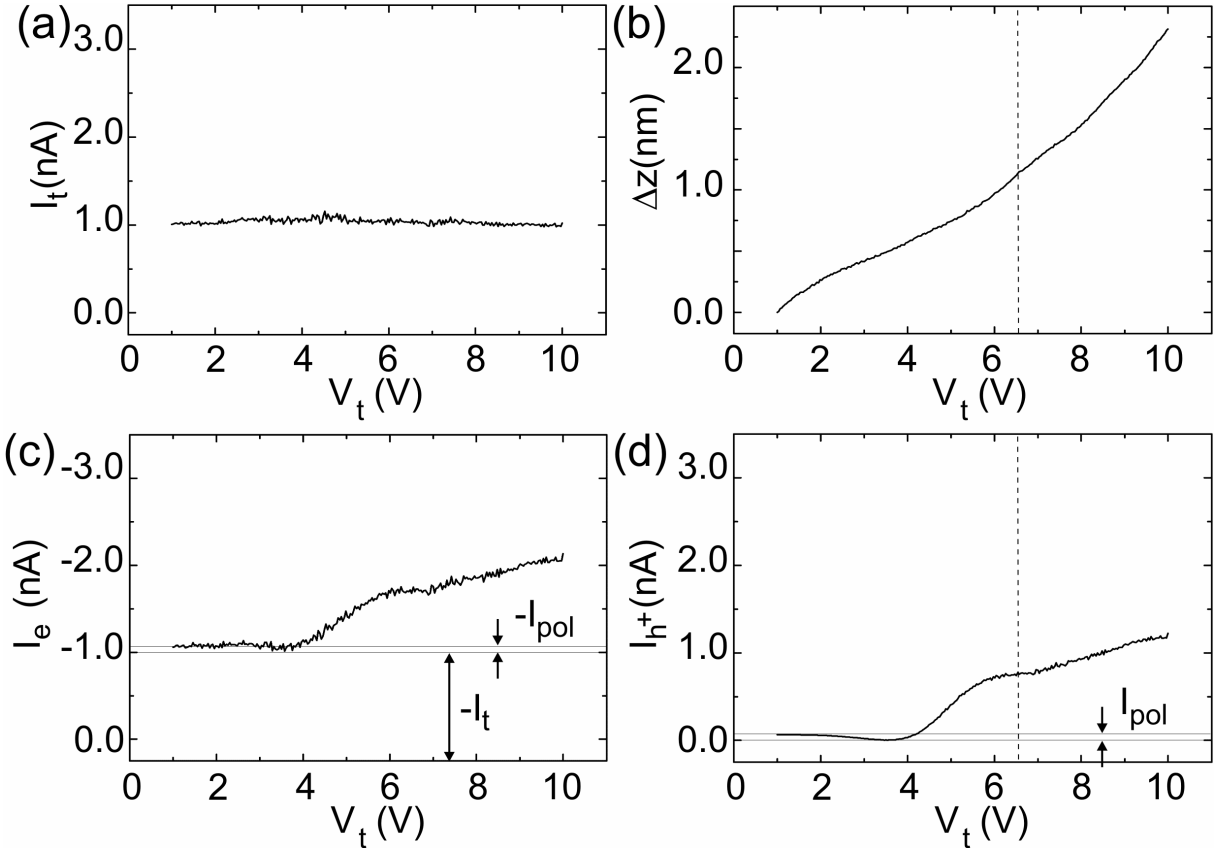

Figure S2: Simultaneous measurement in closed loop of (a) the tunneling current spectrum, (b) the tip-sample separation spectrum, (c) the electron current (I_{e-}) spectrum and (d) the hole current (I_{h+}) spectrum acquired with tips 3, 1 and 2 respectively. The measurement was performed in the space charge layer. The contribution of the tunneling current I_t and polarization current I_{pol} of the diode in reverse bias are indicated in I_{e-} and I_{h+} spectra. The vertical dashed line shows the voltage at which the first field emission resonance occurs.

- The STM tip causes a band bending in the semiconductor. To account for that effect, we have performed simulations of the tip induced band bending and estimated the amount of band bending when impact ionization starts. The plots in Figure S3 are the results of iterative self-consistent solution of the Poisson and Schrödinger equations for the space-charge region at the semiconductor surface. A finite difference technique is used by which the electrostatic problem of a probe tip in proximity to a semiconductor is solved assuming circular symmetry and using prolate spheroidal coordinates in the vacuum.[7] The graph in Figure S3 corresponds to a donor concentration of 4.5×10^{16} As.cm^{-3} and a density of surface states of 10^{14} cm^{-2}, a value consistent with the density of Si dangling bonds and point defects at the surface. It shows the semiconductor surface potential as a function of tip 3 bias for two tip-sample

separations, because of the tip withdrawal as the bias increases during the spectroscopic measurements. At a small tip sample separation of 0.8 nm, the surface potential is 0.18 eV at zero volt and the bands bend upward over a depth of 200 nm into the semiconductor. Raising tip 3 bias shifts the surface potential to 0.40 eV. But as the tip withdraws by 1.2 nm during the measurement as shown in Figure S2b, the band bending becomes smaller and reaches 0.27 eV at a bias of 4V. In conclusion, the surface states provide a strong pinning of the Fermi level at the surface and the upward change of the band bending due to an increase of tip 3 bias is relatively small in comparison with the voltage threshold for impact ionization (4.00 eV). From these simulations, we estimate the energy threshold for impact ionization with respect to the conduction band edge of Si to be 3.63 eV.

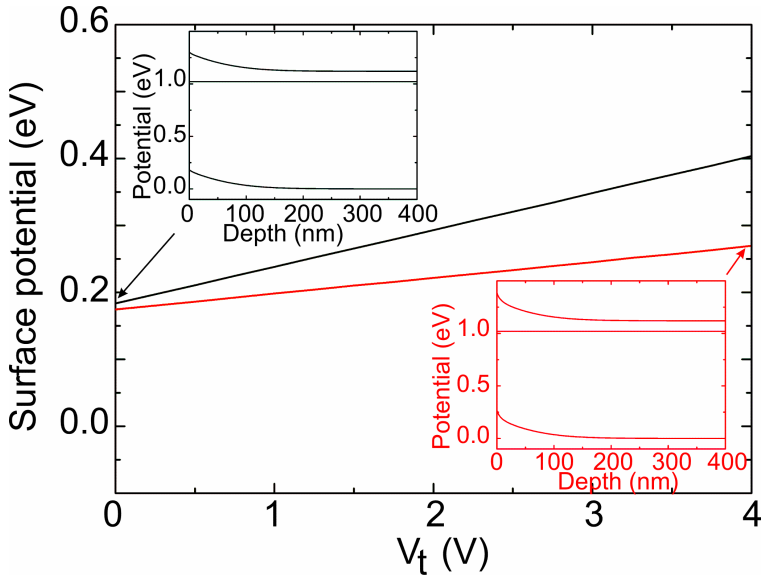

Figure S3: Calculated surface potential induced by the STM tip at the surface of the Si(100) surface in the n-type layer doped with an As concentration of 4.5 x 10^{16} atoms.cm^{-3} as a function of the tip voltage for two different tip-sample separations of 0.8 and 2.0 nm. Insets: Related tip-induced band bending along the depth of the Si crystal. The horizontal line marks the position of the Fermi level.

- Although the presence of the metallic tip induces a band bending, this long range potential is not expected to change the impact ionization rate. The reason is that the long-range potential V induced by the tip varies slowly in space. Therefore the matrix element $\langle \varphi_{c1} \varphi_v | V | \varphi_{c2} \varphi_{c3} \rangle$ for the impact ionization process $(c_1 \rightarrow c_2, v \rightarrow c_3)$ where *c* (*v*) denotes conduction (valence) levels is very small between orthogonal wave-functions characterized by high-*k* components for excited states.

REFERENCES

(1) Coffinier, Y.; Olivier, C.; Perzyna, A.; Grandidier, B.; Wallart, W. ; Durand, J.-O.; Melnyk, O.; Stiévenard, D. *Langmuir* **2005**, *21*, 1489-1496.

(2) Taurus-Process, Version Z-2007.03, Synopsys, Inc.

(3) Robinson, M. T.; Torrens, I. M. *Phys. Rev. B* **1974**, *9*, 5008-5024.

(4) Berthe, M.; Durand, C.; Xu , T.; Nys, J. P.; Caroff, P.; Grandidier, B. Combined STM and Four-Probe Resistivity Measurements on Single Semiconductor Nanowires. In: *Atomic Scale Interconnection Machines*; Joachim, C. Ed.; Springer, **2012**.

(5) Bauer, A.; Ludeke, R. *Phys. Rev. Lett.* **1994**, *72*, 928-931.

(6) Lang, N. D.; Yacoby, A.; Imry, Y. *Phys. Rev. Lett.* **1989**, *63*, 1499.

(7) Feenstra, R. M. *J. Vac. Sci. Technol. B* **2003**, *21*, 2080.